Removal of diethyltoluamide, paracetamol, caffeine and triclosan from natural water by photo-Fenton process using powdered zero-valent iron

Jianan Li [a,b], Chaoran Li [b], Naiara de Oliveira dos Santos [b,c], Luiz A.C. Teixeira [c,d], Luiza C. Campos [b,*]

[a] School of Environmental and Municipal Engineering, Qingdao University of Technology, Qingdao 266520, China
[b] Department of Civil, Environmental & Geomatic Engineering, Faculty of Engineering, University College London, London WC1E 6BT, UK
[c] Department of Chemical and Materials Engineering, PUC-Rio, 22451-900 Rio de Janeiro, Brazil
[d] Peroxidos do Brasil Ltda - Solvay Group, Brazil

ARTICLE INFO

ABSTRACT

The removal of four pharmaceuticals and personal care products (PPCPs), namely diethyltoluamide (DEET), paracetamol (PAR), caffeine (CAF) and triclosan (TCS) (at a spiked concentration of 25 µg/L), from natural water using the photo (UVC)-Fenton (powdered zero-valent iron, pZVI) process was investigated. The results show that a molar ratio of H_2O_2/pZVI of 2.0, pZVI concentration of 22.4 mg/L and pH of 3.0 maximised the removal of the target compounds at 71.1%, 100%, 64.2% and 87.1%, for DEET, PAR, CAF and TCS, respectively, after 30 min in Fenton (pZVI) process. When this process was coupled with UVC radiation, 29.6%, 80.3%, 3.1% and 88.4% of DEET, PAR, CAF and TCS, respectively, were removed within the first minute, and 99.0%, 100%, 99.5% and 100%, respectively, were removed after 30 min. The pseudo first-order kinetic model best fitted the degradation data of DEET, PAR and CAF (1–20 min); and because 80% of TCS and PAR degraded within the first minutes, it is suggested to explore the kinetics during the initial period. Characterisations of pZVI after the photo-Fenton (pZVI) process indicated the corrosion of the surface of iron powder and the presence of iron oxides and iron hydroxides. Lower removals of nitrate (35–50%), phosphate (<35%) and total organic carbon (TOC, <18%) were observed, which may be attributed to the small H_2O_2/pZVI dosage used. Results of this investigation show that the photo-Fenton (pZVI) process has potential for efficient and cost-effective removal of PPCPs.

1. Introduction

In recent years, the problem of environmental contamination by pharmaceuticals and personal care products (PPCPs) has caused increasing concern worldwide [1,2]. These emerging contaminants have been detected in wastewater, natural water, groundwater, soil, biosolids and other biotopes [3–7]. PPCPs in the environment may pose risks (e.g., toxicity) to human and other creatures and heighten corresponding problems, such as the occurrence of antibiotic resistance genes (ARGs) [8]. Hence, elimination of PPCPs from the environment is a pressing concern for environmental researchers and engineers. Wastewater treatment plants (WWTPs) are considered to be the main sources of PPCPs in the environment [9]. Untreated PPCP compounds from WWTPs enter the environment with the effluent discharged. Various treatment techniques for PPCP removal have been studied, including conventional activated sludge, coagulation, constructed wetland, slow sand filtration, membrane filtration and others, but these treatments vary greatly in their effectiveness in removing PPCP compounds [4,10–13].

The Fenton reaction, an advanced oxidation process (AOP), was discovered in 1894 by H.J.H. Fenton, who found that tartaric acid could be oxidised by hydrogen peroxide activated by ferrous (Fe^{2+}) salts [14]. The Fenton reaction is a homogenous process. During this reaction, the HO· radicals produced are a strong oxidising species that are responsible for the oxidation process (Eq. (1)) [15–17].

$$Fe^{2+} + H_2O_2 \rightarrow Fe^{3+} + HO\cdot + HO^- \tag{1}$$

For treating contaminants, the HO· radicals produced by the Fenton reaction oxidise pollutants into small-molecule compounds and further into carbon dioxide, water and other inorganics [18]. The Fenton process has been proven to be effective in treating water to remove PPCPs [19,20], and the combination of the Fenton process with photolysis
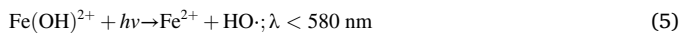
(photo–Fenton) has been reported to enhance the removal efficiency [21–25]. Although proven to be effective, the homogenous Fenton reaction is considered to have some inevitable drawbacks, such as the requirement for large amounts of Fe^{2+} ions (usually from $FeSO_4$), the need for further treatment of iron ions and sludge, and the acidification of effluents before decontamination [26–29].

In recent years, zero-valent iron (ZVI) has been employed to induce Fenton oxidation, and application of ZVI-Fenton for PPCP degradation has been reported in few studies [27,30,31]. Unlike the traditional Fenton process, the ZVI-Fenton reaction process is heterogeneous [32]. During this process, ZVI is corroded and produces Fe^{2+} ions under the presence of H_2O_2 and H^+. The Fe^{2+} react with H_2O_2 to produce reactive oxygen species (ROS), such as HO· radicals, which can degrade PPCP contaminants (Eqs. (2)–(4)) [31,33,34]. Apart from these main reactions, the corrosion of the ZVI surface in water may also occur under aerobic and/or acidic conditions [35,36].

$$Fe^0 + H_2O_2 + 2H^+ \rightarrow Fe^{2+} + 2H_2O \qquad (2)$$

$$Fe^{2+} + H_2O_2 \rightarrow Fe^{3+} + HO\cdot + HO^- \qquad (3)$$

$$2Fe^{3+} + Fe^0 \rightarrow 3Fe^{2+} \qquad (4)$$

Unlike in the conventional Fenton process, both reductive and oxidative reactions can be initiated by the electron transfer on the ZVI surface, making the ZVI-Fenton reaction process more versatile [37]. In addition, recycling of ferric (Fe^{3+}) iron into Fe^{2+} species at the iron surface can also take place as described by Eq. (4) [27]. Other advantages of the ZVI-Fenton process include the production of much less residue and the relatively lower cost compared to the use of ferrous salts, and the recycling and reuse property of ZVI particles [31,38–40].

In recent years, the photo-Fenton (ZVI) process has been investigated to enhance the effectiveness and efficiency of the ZVI-Fenton technique. Ultraviolet (UV) light is typically used for this purpose. Under UV light, the following reactions take place:

$$Fe(OH)^{2+} + h\nu \rightarrow Fe^{2+} + HO\cdot; \lambda < 580 \text{ nm} \qquad (5)$$

$$H_2O_2 + h\nu \rightarrow 2HO\cdot; \lambda < 310 \text{ nm} \qquad (6)$$

Under UV radiation, photolysis of Fe^{3+} cations derived as described by Eq. (3) in acidic media yields Fe^{2+} cations (Eq. (5)), HO· radicals are generated, and regenerated Fe^{2+} cations can react with hydrogen peroxide again (Eq. (3)) [33]. In addition, under radiation at a wavelength of 310 nm, photolysis of hydrogen peroxide into HO· radicals can also occur (Eq. (6)) [16]. Although the overall rates of regeneration and the efficiency of the process described by Eq. (5) are low under radiation [15], additional HO· radicals can be produced, which increases the rate of oxidation.

Nanoparticle zero-valent iron (nZVI) has been employed in some studies using photo-Fenton (ZVI) reaction [28,33,34,41]. However, apart from the high operational costs involved [42], the use of nano-iron particles may also create recycling and after-treatment problems, since filtration of these nanoparticles is difficult [43]. Compared with nano-iron particles, iron powder is cheaper and easier to produce and handle, which makes it a promising alternative. In addition, iron powder was also reported to have good recycling and reuse ability [40]. However, studies in which powdered zero-valent iron (pZVI) has been used in the photo-Fenton reaction have typically focused more on removal of traditional pollutants, such as solvent and nutrients [38,40,44–48]. To the best of our knowledge, pZVI has rarely been used in the photo-Fenton process to remove PPCPs, and no studies have been published on the use of this technique to treat DEET, PAR, CAF or TCS, which are widely detected in the environment and reported to pose potential eco-risks [1,6,49,50]. Therefore, the aim of this work was to optimise the Fenton (pZVI) process parameters for the removal of DEET, PAR, CAF and TCS from natural water. In addition, the removal and degradation kinetic trends during the UVC-Fenton (pZVI) process and the

characteristics of iron powder before and after reaction were examined, using field emission scanning electron microscopy (FESEM) and X-ray photoelectron spectroscopy (XPS).

2. Materials and methods

2.1. Chemicals and materials

Standards and chemicals of DEET, PAR, CAF and TCS were purchased from Sigma-Aldrich (UK). The properties of the four compounds are shown in Table S1 (Appendix A). Methanol and acetonitrile (HPLC grade) were purchased from Fisher Scientific (UK). A stock solution of 1 mg/mL mixed target compounds prepared in methanol was stored at −20 °C and added to natural water to reach a spiked concentration of 25 μg/L throughout the experiment. pZVI (≥99.5%, 5–9 μm) and a hydrogen peroxide solution (50% wt%) were purchased from Sigma-Aldrich (UK) and Fisher Scientific (UK), respectively. pZVI was not submitted to any treatment prior to the experiments. The surface area of pZVI is 0.2988 m^2/g, determined by Brunauer–Emmett–Teller (BET, Quantachrome autosorb-iQ2, USA). A working hydrogen peroxide solution was prepared by diluting the stock solution using ultrapure water (Ondeo Purite IS, UK). In this work, natural water was collected from the Regent's Park Lake, London, UK, which had an average turbidity <2 NTU, a conductivity around 1800 μS/cm, a pH in the range of 7.3 to 7.6 and a TOC concentration of 12.90 ± 0.32 mg/L. The initial concentrations of DEET, CAF and TCS were 1.85 ± 0.14 μg/L, 0.15 ± 0.10 μg/L and 1.32 ± 0.22 μg/L; the concentration of PAR was not detected. Before the experiment, the natural water was filtered through a 0.22-μm cellulose acetate membrane (Whatman, UK).

2.2. Experimental design and procedure

The experiment consisted of the Fenton (pZVI), photo-Fenton (pZVI) and control tests. Fenton (pZVI) tests comprised the optimisation of the H_2O_2/pZVI molar ratio, H_2O_2/pZVI concentration and solution pH. The Fenton (pZVI) test was conducted in batch mode using a shaker (IKA® KS 260, UK) [48]. Samples of 500 mL of natural water at a pH of 3 (adjusted using H_2SO_4 and NaOH in all experiments) [16] and spiked with the target compounds were put into six 600-mL glass bottles and shaken at 270 rpm to ensure thorough mixing. A room temperature of approximately 25 °C was maintained. The shaking was started immediately after pZVI and H_2O_2 were added to the water. The molar ratio tests were conducted using H_2O_2/pZVI ratios of 0.5, 1.0, 1.5, 2.0, 2.5 and 3.0 and a pZVI concentration of 11.2 mg/L (0.2 mmol/L). The concentration tests were conducted using pZVI concentrations of 2.8, 5.6, 11.2, 16.8, 22.4 and 44.8 mg/L and an H_2O_2/pZVI molar ratio of 2.0. For the optimised molar ratio and dosage concentration, removal of the target contaminants was explored with the water pH adjusted to 2.0, 3.0, 4.0, 5.0, 6.0 and 7.0. The reaction times were all 30 min. Control tests involved monitoring the degradation of the target compounds under only H_2O_2 treatment in the dark, at molar concentrations of 0.2, 0.3, 0.4, 0.5 and 0.6 mmol/L.

A schematic representation of the photo-Fenton (pZVI) reactor is shown in Fig. 1. The reactor was similar to the ones used in other photo-Fenton (ZVI) studies [28,34] but air was used to cool the system to maintain 25 °C room temperature instead of water. One 800-mL beaker containing 600 mL of natural water at a pH of 3.0, spiked with the target compounds and with the optimised amounts of pZVI and H_2O_2, was placed in a sealed container made of lightproof plastic. One magnet stirrer was placed at the bottom of the beaker, and a UVC light tube was inserted vertically into the water. Air was pumped at 6.4 L/min into the lower part of the container and flowed out from the upper part to counteract the water temperature generated by the light tube. The reactor was on a magnet stirring machine which stirred at a speed of 120 rpm. The UV lamp used was a UVC monochromatic low-pressure mercury-vapour lamp (11 W, 240 V, 254-nm wavelength, 35 μmol m^{-2} s^{-1}
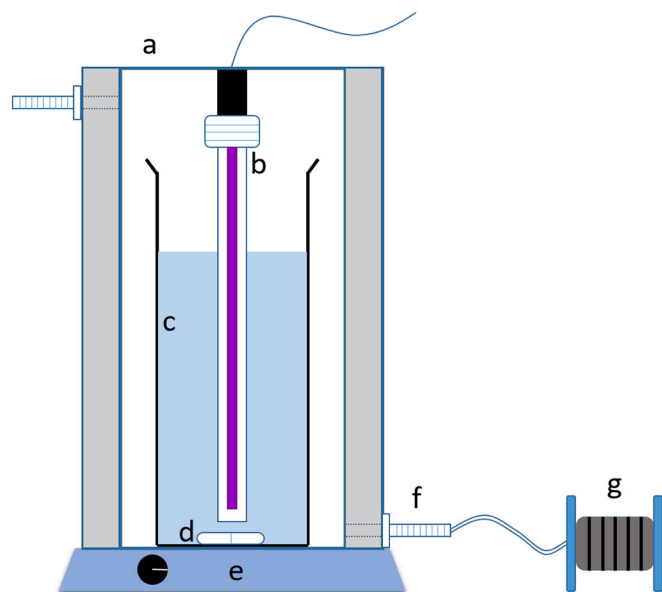
Fig. 1. Schematic representation of the UVC-Fenton (pZVI) reactor (a. PVC plastic container; b. UVC light tube; c. beaker; d. magnet stirrer; e. magnet stirring mixer; f. ventilation hole; g. air pump)

light density, Philips, Holland) [51]. The reaction times in the series of photo-Fenton (pZVI) tests were 1, 3, 5, 10, 15, 20 and 30 min. For the UVC control tests, the experimental solution placed in the beaker without the addition of Fenton (pZVI) was treated under UVC light for 5, 15 and 30 min. All tests above were conducted in triplicates.

2.3. Degradation kinetics

The degradation kinetics of the four target PPCP compounds during the UVC-Fenton (pZVI) process from natural water was modelled using the following pseudo first-order (Eq. (7)) and second-order (Eq. (8)) kinetic models:

$$ln\left(\frac{C_t}{C_0}\right) = -k_1 * t \tag{7}$$

$$\frac{1}{C_t} - \frac{1}{C_0} = k_2 * t \tag{8}$$

where k_1 is the observed pseudo first-order rate constant (min^{-1}) [52], k_2 is the observed second-order rate constant (L/µg·min^{-1}) [53], C_t is the concentration (µg/L) of an individual target compound at time t, and C_0 is the initial concentration (µg/L) of this compound.

To select the better model, apart from the coefficient of correlation (R^2), the sum of the squared errors (SSE) and the Chi-squared statistic (χ^2) error functions were also employed [54–56].

$$SSE = \sum_{i=1}^{n} (q_c - q_e)_i^2 \tag{9}$$

$$\chi^2 = \sum_{i=1}^{n} \left[\frac{(q_c - q_e)^2}{q_e}\right]_i \tag{10}$$

where, q_e and q_c are, respectively, the experimental and calculated target PPCP concentration (µg/L) at time t, and n is the number of experimental data points.

2.4. Characterization of pZVI

After the photo-Fenton (pZVI) experiment, iron powder was

collected in small vials and freeze-dried as soon as possible. The treated iron powder was stored at −20 °C under nitrogen to interrupt the oxidation process. The surface morphology of the pZVI before and after the reaction was characterised using field emission scanning electron microscopy (FESEM, secondary electron detector, accelerating voltage at 20.00 kV, JEOL JSM-6700F, Japan). X-ray photoelectron spectroscopy (XPS, pass energy at 50 eV, monochromatic Al Kα radiation and a 180° double focusing hemispherical analyzer with 128-channel detector, spectrometer Thermo Fisher K-alpha, UK) analysis of the pZVI was performed to characterise its surface chemical composition after the UVC-Fenton (pZVI) reaction. The CasaXPS 2.3.16 software (line shape model: Gaussian-Lorentzian peak function) was used to determine the spectra peaks and conduct the analysis.

2.5. Analytical methods

Solid-phase extraction (SPE) and gas chromatography–mass spectrometry (GC–MS), which are described in detail in our previous studies [11,57], were used for extraction and quantification of the four target compounds from the water. The total organic carbon (TOC) content was determined using a Shimadzu TOC-L machine (UK). Nitrite, nitrate and phosphate concentrations after the pZVI process were measured using ion chromatography (IC, Dionex ICS 1100, US). Removal (%) of the target PPCP compounds were calculated using Eq. (11):

$$\text{Removal (\%)} = \frac{C_i + C_a - C_f}{C_i + C_a} \times 100\% \tag{11}$$

where C_i (µg/L) is the initial concentration of a target compound from natural water, C_a is the added concentration (25 µg/L of each compound) and C_f (µg/L) is the final concentration.

3. Results and discussion

3.1. Fenton (pZVI) process optimisation

The effects of the tested H_2O_2/pZVI molar ratios, H_2O_2/pZVI concentrations and pH values are shown in Fig. 2. As the H_2O_2/pZVI molar ratio increased from 0.5 to 2.0, the removal of the four compounds increased by approximately 30% on average (Fig. 2-A). At a molar ratio of 2.0, the removals were 66.3%, 87.3%, 48.1% and 90.3% for DEET, PAR, CAF and TCS, respectively. DEET is usually regarded as a more recalcitrant compound than CAF in biological treatments [11,58]. However, the results here indicate that the H_2O_2/pZVI-Fenton process may be a better choice for degrading DEET than for degrading CAF. As in the case of the traditional H_2O_2/Fe^{2+} process, for which the range of reported optimal ratios is wide (2.5–20) [19,59], the reported range of optimal H_2O_2/ZVI molar ratios for treating emerging contaminants and other phenolic compounds is also wide (0.25–10) [31,52,60]. In the present study, the optimal H_2O_2/pZVI molar ratio was found to be 2.0. However, when the molar ratio was increased from 2.0 to 3.0, the removal decreased slightly for all four compounds. This may be attributed to the scavenging effects of H_2O_2 on HO· radicals and the formation of radicals with lower oxidative potential (Eqs. (12) and (13)) [15]:

$$H_2O_2 + HO· \rightarrow HO_2· + H_2O \tag{12}$$

$$HO_2· + HO· \rightarrow H_2O + O_2 \tag{13}$$

The scavenging process may consume the HO· radicals generated, and because $HO_2·$ is less reactive, this may account for the decreased removal observed. Furthermore, the inhibition of pZVI corrosion by high concentration of H_2O_2 may also cause the removal decline [26,31,61]. The results of the control tests using H_2O_2 only without light radiation and pZVI are shown in Fig. S1 (Appendix A). Because of the oxidising property of hydrogen peroxide, it is also used to treat refractory organic substances in wastewater [62]. For various concentrations of hydrogen
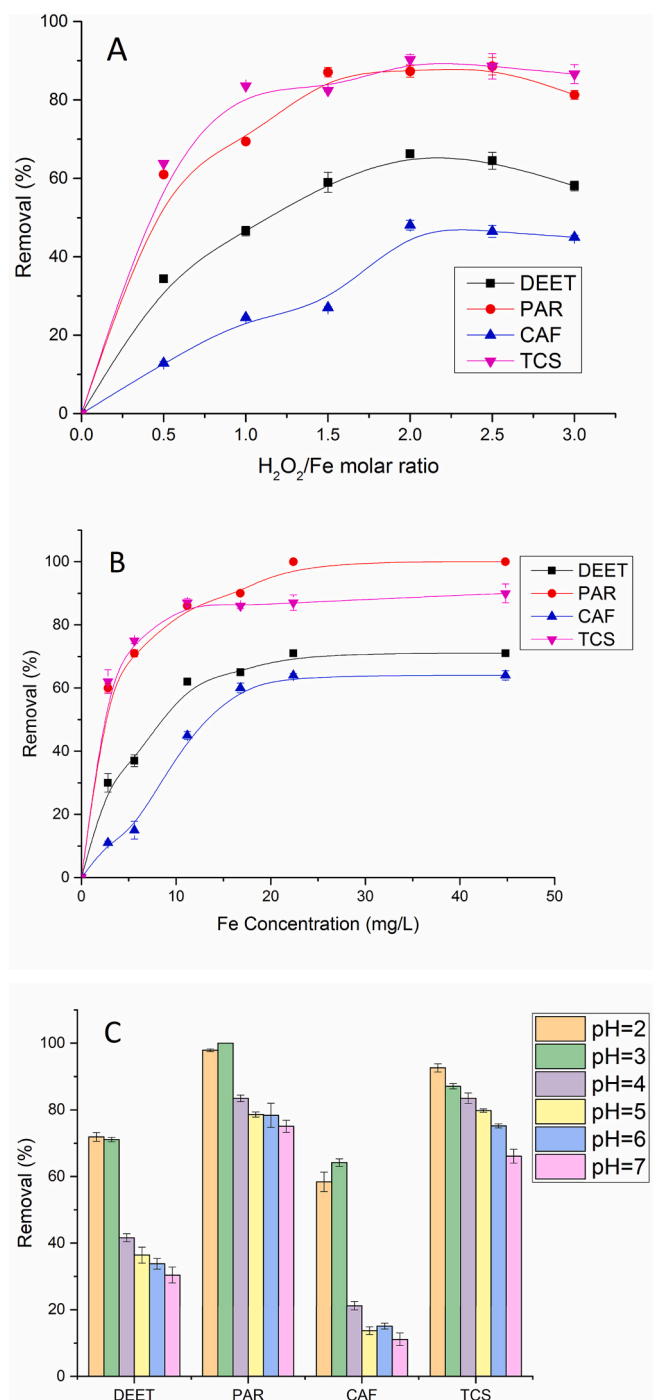
(pZVI) process played a significant degradation role. However, the removal of the four compounds did not increase linearly with the H_2O_2 dose. Since H_2O_2/pZVI process is heterogenous, limited pZVI surface sites and the inhibition of pZVI corrosion by high concentration of H_2O_2 may also restrict the overall performance when excessive H_2O_2 was added into the system, leading to inhibition of the oxidative transformation pathways [31,63]. In addition, H_2O_2 may also be involved in other parallel reactions such as its self-decomposition [64] (Eq. (14)):

$$2H_2O_2 \rightarrow O_2 + 2H_2O \tag{14}$$

The removal results for various H_2O_2/pZVI concentrations at a molar ratio of 2.0 are shown in Fig. 2-B. As the concentration of spiked pZVI increased from 2.8 to 44.8 mg/L (0.05 to 0.4 mmol/L), the removal of all four compounds initially increased rapidly and then more slowly. This phenomenon has also been reported by other researchers [26,41]. As the pZVI concentration increased from 22.4 mg/L to 44.8 mg/L, the removal increased by less than 3%. Apart from the H_2O_2/pZVI reaction, scavenging of HO· radicals by H_2O_2 (Eq. (12)) and decomposition of H_2O_2 (Eq. (14)) can also occur in the aqueous phase simultaneously [65], which means that H_2O_2 cannot exist in water for a long time. In addition, whereas the H_2O_2/Fe^{2+} process is homogeneous, the H_2O_2/pZVI reaction is heterogeneous. With the oxidation of the target compounds, their remaining concentrations gradually decrease, leading to slowing of the reaction, as the pZVI particles cannot remain uniformly distributed in the water, and other substances may compete for the oxidising radicals [34]. However, the residual H_2O_2 concentration was not measured in this study, and the possible explanation offered above is a speculation that needs to be investigated. At a pZVI concentration of 44.8 mg/L, the final removals of DEET, PAR, CAF and TCS were 72.1%, 100%, 66.2 and 87.5%, respectively. Unequal removal for different emerging contaminants have also been reported elsewhere [19] and can be explained by the properties of the compound structure and the competition for reactive ZVI sites with other substances in water [16,20,61]. Although the removal at a pZVI concentration of 44.8 mg/L were slightly higher than those at 22.4 mg/L, exploitation of bulk oxidant can lead to an unnecessary treatment cost increase [66]. Hence, 22.4 mg/L was chosen as the optimal pZVI concentration.

The conventional Fenton process is greatly influenced by the reaction pH [15]. The optimal initial pH value is typically approximately 3 [16,67–69], but some studies have reported achievement of satisfactory results at higher pH values (e.g., approximately 7) [70–72]. Therefore, in the present study, the removals of the four target compounds at initial pH values of 2.0, 3.0, 4.0, 5.0, 6.0 and 7.0 were investigated (Fig. 2-C). Due to small reagents dosage, no obvious pH changes of solution were measured after all reactions. As with the aforementioned results, higher removals were achieved for PAR and TCS than for the other two compounds over the full range of pH values considered. In general, PPCP removals decreased with increasing pH, with the highest removals (71.1%, 100%, 64.2% and 87.1% for DEET, PAR, CAF and TCS, respectively) achieved at a pH of 3.0. At a pH of 7.0, removals were much lower (30.4%, 75.1%, 11.1% and 66.1%, respectively) than at pH of 3. The decreased degradation performance at higher pH values may be attributed to the decomposition of H_2O_2, the lower oxidation potential of HO· radicals, and the formation of ferric hydroxide complexes [26]. In addition, the corrosion of iron also decreases with increasing pH and weaker oxidants such as ferryl ion may be generated rather than Fe^{3+} (Eq. (15)) at pH above 5, which is more selective than HO· [26,31].

$$Fe^{2+} + H_2O_2 \rightarrow Fe\ (IV)\ \left(e.g. FeO^{2+}\right) + H_2O \tag{15}$$
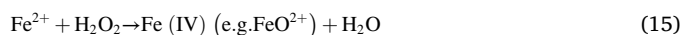
All these possibilities may negatively affect the oxidation process. However, it should be noted that no significant differences ($p > 0.05$, t-test) in removal were observed for pH values of 2.0 versus 3.0, although at a pH of 3.0, the removals of PAR and CAF were both 6% lower, whereas those for DEET and TCS were slightly higher (0.8% and 5.5%, respectively). At a very low pH (e.g., pH ≤ 2), concentration decline of

Fig. 2. Removal of DEET, PAR, CAF and TCS under various H_2O_2/pZVI molar ratio, H_2O_2/pZVI concentration and sample pH (n = 3) (A. Different H_2O_2/pZVI molar ratio. Target compounds concentration = 25 μg/L, pZVI concentration = 11.2 mg/L, pH = 3, 25 °C; B. Different H_2O_2/pZVI concentration. Target compounds concentration = 25 μg/L, H_2O_2/pZVI molar ratio = 2.0, pH = 3, 25 °C; C. Different solution working pH. Target compounds concentration = 25 μg/L, H_2O_2/pZVI molar ratio = 2.0, pZVI concentration = 22.4 mg/L, 25 °C).

peroxide, no obvious differences in removal were observed, with average removal of approximately 20% for both DEET and TCS and a removal of approximately 60% for PAR. Removal of CAF was negligible, indicating that CAF is difficult to degrade using H_2O_2. Compared to the control tests, the H_2O_2/pZVI tests achieved higher removal, especially for CAF (an increase from 10% to 50% when H_2O_2 was combined with pZVI) (Fig. 2), suggesting that HO· radicals generated during the Fenton

the Fe(OH)$^{2+}$ may negatively affect pZVI performance. Furthermore, H_2O_2 is more stable at low pH because of the formation of $H_3O_2^+$, which limits the generation of HO· radicals [15]. For this reason, although the removal of the target compounds was similar at pH values of 2 and 3, a pH of 3 was selected as the optimal initial pH.

3.2. Removal of target PPCP compounds under UVC-Fenton pZVI process

The removal results achieved with the UVC-Fenton pZVI process are shown in Fig. 3. Oxidation starts to occur immediately upon commencement of the test. After only 1 min, 29.6%, 80.3%, 3.1% and 88.4% of the DEET, PAR, CAF and TCS, respectively, were removed. For the results reported above for the Fenton (pZVI) experiment, although the removals of DEET and CAF were lower than those for PAR and TCS, after 30 min, the removals achieved were 99.0%, 100%, 99.5% and 100% for DEET, PAR, CAF and TCS, respectively, demonstrating the excellent performance of the treatment. The results of the control tests conducted using only UVC are also shown in Fig. 3. Under UVC, higher removals were achieved for PAR and TCS than for DEET and CAF. After 30 min, 50.0%, 90.0%, 24.3% and 93.9% removals were observed for DEET, PAR, CAF and TCS, respectively. The higher removals for PAR and TCS than for DEET and TCS are consistent with results reported for tests conducted under natural light [57]. It has also reported that light can favour the photo-degradation of PAR and TCS [73–76]. As the UVC has greater energy than natural visible light, more HO· radicals could be generated, according to Eq. (6). Therefore, photo-degradation of light-sensitive compounds should be more rapid under UVC. The DEET, PAR, CAF and TCS removals under UVC (35 μmol m^{-2} s^{-1}) after just 5 min (30.0%, 74.0%, 10.3% and 90.3%, respectively) were notably higher than those observed under natural light (240 μmol m^{-2} s^{-1}) for 7 days (1.2%, 46.2%, −1.1% and 57.6%, respectively) [57].

The pseudo first-order kinetic model has been widely reported as describing the degradation process of chemicals in the Fenton, Fenton-like and photo-Fenton processes well [26,77,78]. The second-order kinetic model has also been used to describe the Fenton and photo-Fenton degradation processes [79]. Because the total removal of PAR and TCS at 30 min led to the inapplicability of the two models and above 80% of them were removed within the first minute, to ensure the consistency, the models were fitted using only observations from 1 to 20 min. The results of R^2, SSE and χ^2 showed the best fitting trends of DEET, PAR and

CAF by pseudo first-order models, while second-order kinetic model best described the TCS degradation trend in the present system (Tables 1 and S2, Appendix A). The fitted R^2 values of DEET, PAR and CAF using pseudo first-order models were 0.9963, 0.9856 and 0.9876, compared to the second-order kinetic models with R^2 values of 0.9255, 0.7864 and 0.9005, respectively. In contrast, the R^2 values of TCS using pseudo first-order and second-order kinetic models were 0.8732 and 0.9092, respectively, and a second-order model usually implies that the degradation of a compound is controlled by its initial concentration [79]. It should be noted that the kinetic fittings did not include the first minute. As Fig. 3 shows, most of the PAR and TCS (>80%) were degraded within the first minute, indicating the degradation kinetics of them during this period may be different from the latter period. However, a short reaction period of 1 min makes sampling relatively difficult and less precise. Therefore, further investigation into the very early stage of PAR and TCS degradation is recommended under other test conditions (e.g., at a very low temperature) to obtain a better understanding of the rapid degradation kinetic trends involved.

Field emission scanning electron microscopy (SEM) images obtained before and after the UVC-Fenton (pZVI) reaction are shown in Fig. 4 and confirm the spherical shape of pZVI particle aggregates before the reaction. After the reaction, corrosion was found on the pZVI surface, and aggregation of small-scale clusters and cotton-like structures were observed. The corrosion of the pZVI identified after the pZVI reaction confirms the surface oxidation of pZVI, which led to the leaching of Fe^{2+} and Fe^{3+} from the pZVI surface. Those iron ions are responsible to react with H_2O_2 and UV radiation to produce ROS for further reactions [31,78]. The SEM images also demonstrate that corrosion did not deplete all pZVI particles and the pZVI in the tested system was sufficient.

(Top left: pZVI before UVC-Fenton process, ×1500 folds; top right: pZVI before UVC-Fenton process, ×8000 folds; bottom left: pZVI after UVC-Fenton process, ×1500 folds; bottom right: pZVI after UVC-Fenton process, ×8000 folds. Red circles indicate obvious corrosion)

X-ray photoelectron spectroscopy (XPS) was used to study the surface chemical composition of the pZVI after the UVC-Fenton (pZVI) reaction. The original spectra are shown in Fig. S2 (Appendix A). Fig. 5 shows the Fe2p core-level spectrum. The two Fe2p$_{3/2}$ and Fe2p$_{1/2}$ peaks in the Fe2p spectrum at binding energies around 710 eV and 724–725 eV, with shake-up satellite peaks at around 719.1 eV and 733 eV,
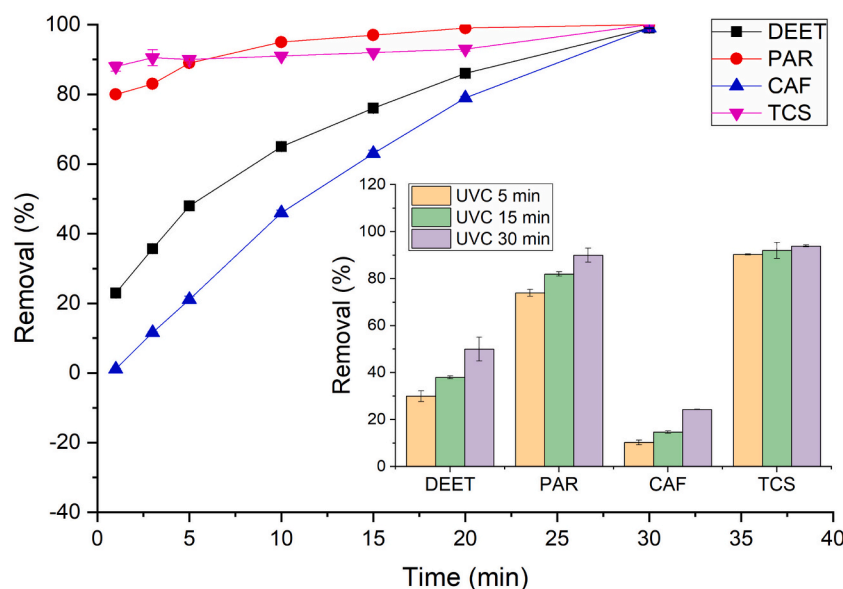

Fig. 3. Removal of DEET, PAR, CAF and TCS under UVC-Fenton pZVI process, and removal results using only UVC (n = 3) (Conditions: Target compounds concentration = 25 μg/L, H_2O_2/pZVI molar ratio = 2.0, pZVI concentration = 22.4 mg/L, pH = 3, 25 °C, reaction time = 30 min; background concentrations of DEET, PAR, CAF and TCS were 1.85 ± 0.14 μg/L, 0, 0.15 ± 0.10 μg/L and 1.32 ± 0.22 μg/L, respectively).

Table 1

Fitting parameters of the kinetic models of the pseudo first-order and second-order equations for degradation of DEET, PAR, CAF, and TCS during the UVC-Fenton (pZVI) process (1–20 min).

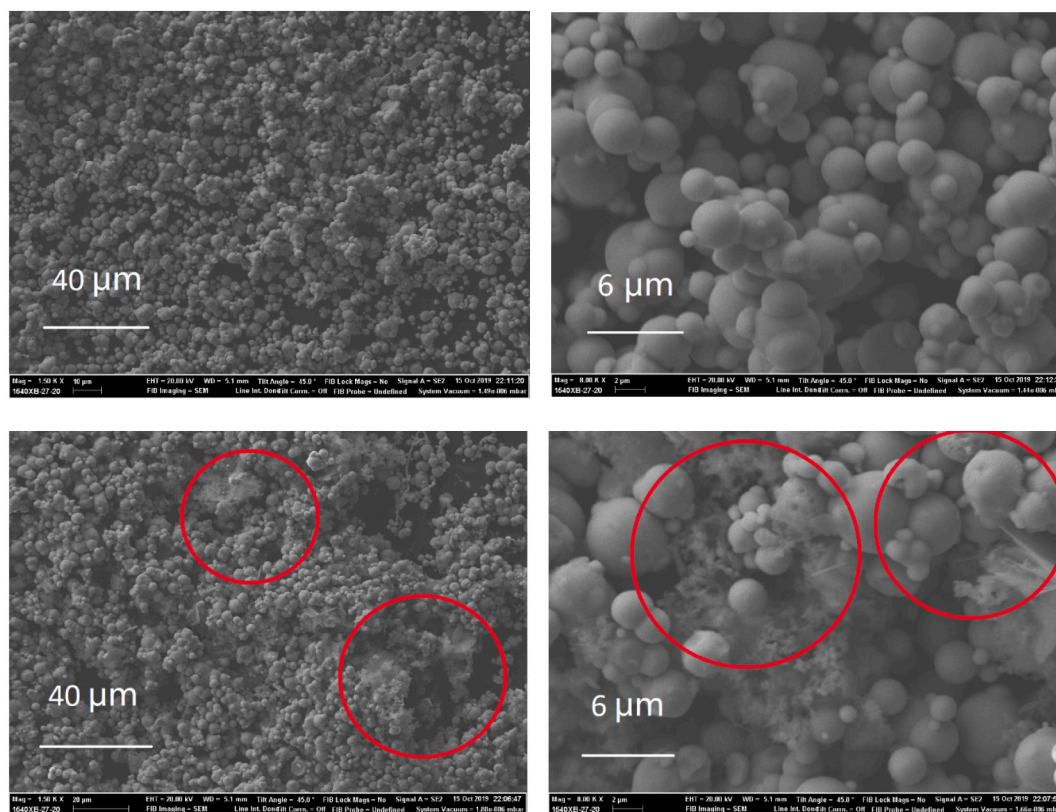| Compound	Pseudo first-order			Second-order		
	Regression equation	k_1 (min^{-1})	R^2	Regression equation	k_2 (L/µg·min^{-1})	R^2
DEET	y = −0.0872x − 0.1792	0.0872	0.9963	y = 0.0115x + 0.0222	0.0115	0.9255
PAR	y = −0.1556x − 1.3880	0.1556	0.9856	y = 0.1824x − 0.4617	0.1824	0.7864
CAF	y = −0.0803x + 0.1316	0.0803	0.9876	y = 0.0074x + 0.0184	0.0074	0.9005
TCS	y = −0.0243x − 2.1713	0.0243	0.8732	y = 0.0108x + 0.3457	0.0108	0.9092

Fig. 4. SEM images of pZVI before and after UVC-Fenton (pZVI) process.

indicate the presence of Fe^{3+} ions [80]. A peak-differentiating analysis was also conducted for the 710 eV binding energy peak, which is displayed in the small inset graph in Fig. 5. After differentiating the peak, binding energies of around 709.6 eV, 710.8 eV and 711.8 eV, corresponding to FeO, Fe_2O_3 and FeOOH, respectively, were found. These results are consistent with findings reported elsewhere [81], and the spectrum indicates that iron oxides and iron hydroxides existed, which is also consistent with the corrosion phenomenon shown by the SEM images [31,44,81,82]. To confirm the oxygen species surrounding the iron ions, O1s core level spectra were also differentiated (Fig. 6). Two peaks, at binding energies of around 530.3 eV and 531.5 eV, were found, demonstrating the presence of lattice oxygen O_2^- and $^-$OH species [80], which further confirms the presence of iron oxides and iron hydroxide.

3.3. General water parameters during UVC-Fenton (pZVI) process

The concentrations of nitrite, nitrate, phosphate and TOC during the UVC-Fenton (pZVI) process are shown in Table 2. Nitrite was totally removed after the treatment. The removal of nitrate fluctuated between 35% and 50%, which is a lower range than that of 50–68% reported elsewhere for a higher concentration (g/L level) of ZVI nanoparticles [83]. Because nitrate can only be reduced to nitrite while HO· radicals

can oxidise nitrite into nitrate, the decreases in the concentrations of nitrite and nitrate can only be attributed to the reduction reaction by pZVI [45,61,83]. In comparison, lower phosphate removal was achieved. For an initial phosphate concentration of 1.73 ± 0.01 mg/L, final phosphate concentrations of 1.13 to 1.73 mg/L (<35% reduction) were detected. In this process, phosphate removal is largely attributed to electrostatic adsorption and surface complexation of phosphate onto the iron powder surface [84]. Competition for iron active sites and adsorption/desorption may lead to this low removal and fluctuation of the concentration. The TOC concentration decreased gradually from an initial value of 12.90 ± 0.32 mg/L to 10.58 ± 0.13 mg/L (after 30 min), or 18% removal. Other researchers have reported achieving TOC removals greater than 60% using photo-Fenton (ZVI) processes [28,34,38] or solely Fenton (ZVI) processes [26,27,80,85]. The higher TOC removal achieved in other studies can be attributed to the higher H_2O_2/pZVI doses (g/L concentration compared to 0.8 mmol/L H_2O_2), longer reaction times (60 min or hours compared to 30 min), and/or higher reagent concentration ratios (e.g. H_2O_2/ZVI at 60, compared to 2.0) used in those studies. In studies in which iron nails (cuts) have been employed to conduct H_2O_2/ZVI processes, up to 100% removal of humic acids (from an initial concentration of 10 mg/L) from pure water within 60 min and around 50–60% removal of dissolved organic carbon (from an initial
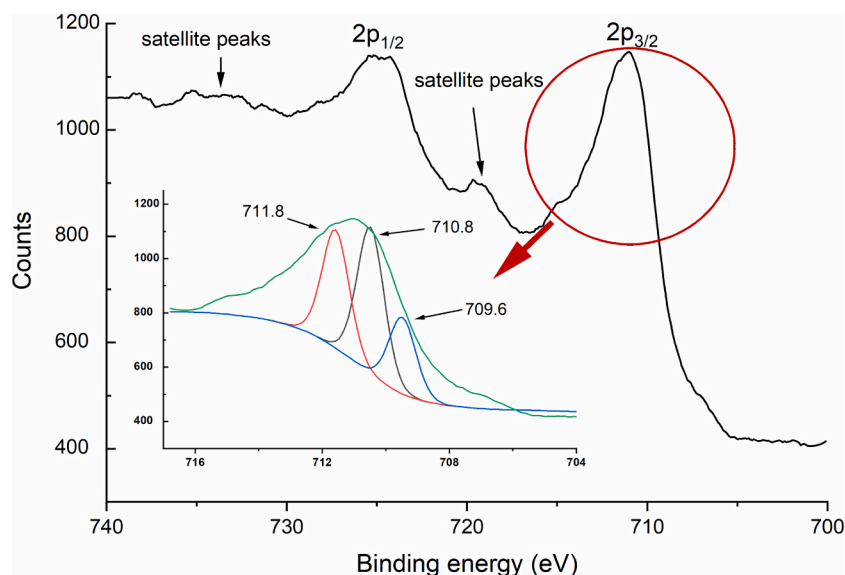
Fig. 5. The XPS spectra of pZVI after the UVC-Fenton (pZVI) process (Savitzky-Golay method used to smooth the original spectrum. Number of points: 10).
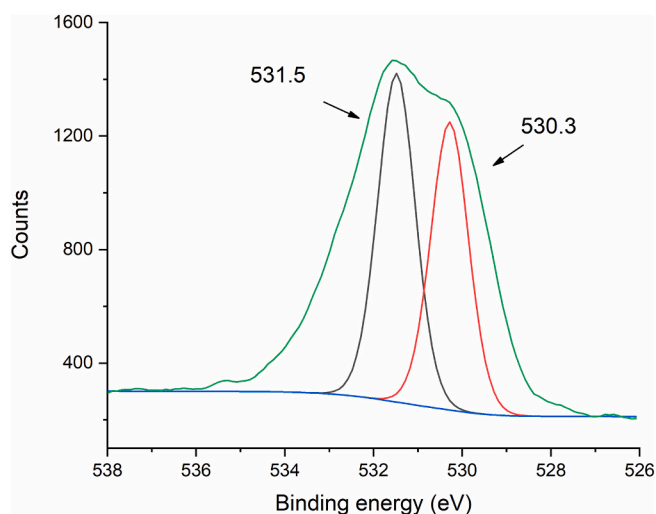

Fig. 6. O1s core level spectra after the UVC-Fenton (pZVI) process (Savitzky-Golay method used to smooth the original spectrum. Number of points: 10).

Table 2
Concentrations of nitrite, nitrate, phosphate and TOC during the UVC-Fenton (pZVI) process (n = 3).

	Nitrite		Nitrate		Phosphate		TOC	
	Con (mg/L)	RSD	Con (mg/L)	RSD	Con (mg/L)	RSD	Con (mg/L)	RSD
Initial	0.21	0.01	8.88	1.82	1.73	0.01	12.90	0.32
1 min	n.d.*	n.a.**	5.54	0.18	1.13	0.06	12.33	0.02
3 min	n.d.	n.a.	5.15	0.07	1.33	0.08	12.26	0.01
5 min	n.d.	n.a.	4.58	0.23	1.69	0.11	12.21	0.07
10 min	n.d.	n.a.	4.91	0.06	1.73	0.04	11.97	0.01
15 min	n.d.	n.a.	5.69	1.15	1.59	0.28	11.76	0.05
20 min	n.d.	n.a.	5.67	1.45	1.40	0.07	11.32	0.04
30 min	n.d.	n.a.	5.76	0.03	1.24	0.03	10.58	0.13

* Not detected. ** Not available.

concentration around 5 mg/L) from natural water within 60 or 75 min have been achieved, but the iron dosages were 50 g/L [86–88]. Despite insufficient TOC mineralisation observed at a low H_2O_2/pZVI reagent dosage, the high removals of the target PPCP compounds achieved in the present study suggest the suitability of this method for treating water for emerging contaminants. Nonetheless, it is also suggested to investigate the TOC mineralisation in the Fenton process optimisation period, as well as relevant control tests, to compare the contributions of various TOC removal pathways.

Examination of the degradation products of the tested PPCP compounds created during the photo-Fenton (pZVI) process was not within the scope of the present study. Degradation pathways are typically explored when a single compound is studied. Although it would be more complex, it would also be meaningful to examine the degradation pathways of the by-products of mixed target compounds during the photo-Fenton (pZVI) process. Besides, other aspects, such as the investigation of pZVI adsorption effect for PPCPs, will further help understanding the mechanisms.

4. Conclusion

In the present study, the removal of four PPCP compounds (DEET, PAR, CAF and TCS) from natural water (spiked concentration at 25 µg/L) using the photo (UVC, 35 µmol m^{-2} s^{-1} light density)-Fenton (pZVI) process was investigated and optimised. A molar ratio of H_2O_2/pZVI of 2.0, pZVI concentration of 22.4 mg/L, and sample pH of 3.0 maximised the removal of the target compounds from natural water at 71.1%, 100%, 64.2% and 87.1% for DEET, PAR, CAF and TCS, respectively. When coupled with UVC radiation, the process removed 99.0%, 100%, 99.5% and 100% of DEET, PAR, CAF and TCS, respectively, after 30 min. After the photo-Fenton (pZVI) process, corrosion of the surface of iron powder and the presence of iron oxides and iron hydroxides were observed. The pseudo first-order kinetic model best fitted ($R^2 > 0.98$) the degradation data of DEET, PAR and CAF (1–20 min) and the rapid elimination of TCS and PAR during the first minute of the reaction suggested the need for investigation into their behaviours and kinetics during the early degradation stage. However, lower removals of nitrate, phosphate and TOC from natural water were detected using the photo-Fenton (pZVI) process, which may be attributed to the small H_2O_2/pZVI reagent dosage used in this study.

Declaration of competing interest

The authors declare that they have no known competing financial interests or personal relationships that could have appeared to influence the work reported in this paper.

Appendix A. Supplementary data

Supplementary data to this article can be found online at https://doi.org/10.1016/j.jwpe.2022.102907.

References

[1] V. Singh, S. Suthar, Occurrence, seasonal variation, mass loading and fate of pharmaceuticals and personal care products (PPCPs) in sewage treatment plants in cities of upper Ganges bank, India, J. Water Process Eng. 44 (2021), 102399, https://doi.org/10.1016/j.jwpe.2021.102399.

[2] P. Chaturvedi, P. Shukla, B.S. Giri, P. Chowdhary, R. Chandra, P. Gupta, A. Pandey, Prevalence and hazardous impact of pharmaceutical and personal care products and antibiotics in environment: a review on emerging contaminants, Environ. Res. 194 (2021), 110664, https://doi.org/10.1016/j.envres.2020.110664.

[3] J. Li, W. Cheng, L. Xu, P.J. Strong, H. Chen, Antibiotic-resistant genes and antibiotic-resistant bacteria in the effluent of urban residential areas, hospitals, and a municipal wastewater treatment plant system, Environ. Sci. Pollut. Res. 22 (2015) 4587–4596, https://doi.org/10.1007/s11356-014-3665-2.

[4] S. Zhang, S. Gitungo, L. Axe, J.E. Dyksen, R.F. Raczko, A pilot plant study using conventional and advanced water treatment processes: evaluating removal efficiency of indicator compounds representative of pharmaceuticals and personal care products, Water Res. 105 (2016) 85–96, https://doi.org/10.1016/j.watres.2016.08.033.

[5] W. Cheng, J. Li, Y. Wu, L. Xu, C. Su, Y. Qian, Y.G. Zhu, H. Chen, Behavior of antibiotics and antibiotic resistance genes in eco-agricultural system: a case study, J. Hazard. Mater. 304 (2016) 18–25, https://doi.org/10.1016/j.jhazmat.2015.10.037.

[6] N.J.D.G. Reyes, F.K.F. Geronimo, K.A.V. Yano, H.B. Guerra, L.H. Kim, Pharmaceutical and personal care products in different matrices: occurrence, pathways, and treatment processes, Water (Switzerland). 13 (2021) 1159, https://doi.org/10.3390/w13091159.

[7] D. Sadutto, V. Andreu, T. Ilo, J. Akkanen, Y. Picó, Dataset of pharmaceuticals and personal care products in a Mediterranean coastal wetland, Data Br. 36 (2021), 116353, https://doi.org/10.1016/j.dib.2021.106934.

[8] J. Li, W. Cheng, L. Xu, Y. Jiao, S.A. Baig, H. Chen, Occurrence and removal of antibiotics and the corresponding resistance genes in wastewater treatment plants: effluents' influence to downstream water environment, Environ. Sci. Pollut. Res. 23 (2016) 6826–6835, https://doi.org/10.1007/s11356-015-5916-2.

[9] H. Chen, X. Li, S. Zhu, Occurrence and distribution of selected pharmaceuticals and personal care products in aquatic environments: a comparative study of regions in China with different urbanization levels, Environ. Sci. Pollut. Res. 19 (2012) 2381–2389, https://doi.org/10.1007/s11356-012-0750-2.

[10] Q. Sui, J. Huang, S. Deng, W. Chen, G. Yu, Seasonal variation in the occurrence and removal of pharmaceuticals and personal care products in different biological wastewater treatment processes, Environ. Sci. Technol. 45 (2011) 3341–3348, https://doi.org/10.1021/es200248d.

[11] J. Li, X. Han, B.W. Brandt, Q. Zhou, L. Ciric, L.C. Campos, Physico-chemical and biological aspects of a serially connected lab-scale constructed wetland-stabilization tank-GAC slow sand filtration system during removal of selected PPCPs, Chem. Eng. J. 369 (2019) 1109–1118, https://doi.org/10.1016/j.cej.2019.03.105.

[12] S.O. Ganiyu, E.D. Van Hullebusch, M. Cretin, G. Esposito, M.A. Oturan, Coupling of membrane filtration and advanced oxidation processes for removal of pharmaceutical residues: a critical review, Sep. Purif. Technol. 156 (2015) 891–914, https://doi.org/10.1016/j.seppur.2015.09.059.

[13] M.F.M.A. Zamri, R. Bahru, A.H. Shamsuddin, S.K. Pramanik, I.M.R. Fattah, F. Suja, Treatment strategies for enhancing the removal of endocrine-disrupting chemicals in water and wastewater systems, J. Water Process Eng. 41 (2021), 102017, https://doi.org/10.1016/j.jwpe.2021.102017.

[14] H.J.H. Fenton, LXXIII., Oxidation of tartaric acid in presence of iron, J. Chem. Soc. Trans. 65 (1894) 899–910, https://doi.org/10.1039/CT8946500899.

[15] J. Herney-Ramirez, M.A. Vicente, L.M. Madeira, Heterogeneous photo-Fenton oxidation with pillared clay-based catalysts for wastewater treatment: a review, Appl. Catal. B Environ. 98 (2010) 10–26, https://doi.org/10.1016/j.apcatb.2010.05.004.

[16] S. Rahim Pouran, A.R. Abdul Aziz, W.M.A. Wan Daud, Review on the main advances in photo-Fenton oxidation system for recalcitrant wastewaters, J. Ind. Eng. Chem. 21 (2015) 53–69, https://doi.org/10.1016/j.jiec.2014.05.005.

[17] A. Rynkowska, J. Stępniak, M. Karbownik-Lewińska, Fenton reaction-induced oxidative damage to membrane lipids and protective effects of 17β-estradiol in porcine ovary and thyroid homogenates, Int. J. Environ. Res. Public Health 17 (2020) 1–9, https://doi.org/10.3390/ijerph17186841.

[18] N. Huda, A.A. Raman, S. Ramesh, Optimization of electrocoagulation process for the treatment of landfill leachate, IOP Conf. Ser. Mater. Sci. Eng. 210 (2017) 166–174, https://doi.org/10.1088/1757-899X/210/1/012008.

[19] W. Li, V. Nanaboina, Q. Zhou, G.V. Korshin, Effects of Fenton treatment on the properties of effluent organic matter and their relationships with the degradation of pharmaceuticals and personal care products, Water Res. 46 (2012) 403–412, https://doi.org/10.1016/j.watres.2011.11.002.

[20] L.L. Tayo, A.R. Caparanga, B.T. Doma, C.-H. Liao, A review on the removal of pharmaceutical and personal care products (PPCPs) using advanced oxidation processes, J. Adv. Oxid. Technol. 21 (2018) 196–214, https://doi.org/10.26802/jaots.2017.0079.

[21] N. De la Cruz, L. Esquius, D. Grandjean, A. Magnet, A. Tungler, L.F. de Alencastro, C. Pulgarín, Degradation of emergent contaminants by UV, UV/H2O2and neutral photo-Fenton at pilot scale in a domestic wastewater treatment plant, Water Res. 47 (2013) 5836–5845, https://doi.org/10.1016/j.watres.2013.07.005.

[22] F. Méndez-Arriaga, S. Esplugas, J. Giménez, Degradation of the emerging contaminant ibuprofen in water by photo-Fenton, Water Res. 44 (2010) 589–595, https://doi.org/10.1016/j.watres.2009.07.009.

[23] M.M. Ahmed, S. Chiron, Solar photo-Fenton like using persulphate for carbamazepine removal from domestic wastewater, Water Res. 48 (2014) 229–236, https://doi.org/10.1016/j.watres.2013.09.033.

[24] Y. Ahmed, J. Zhong, Z. Yuan, J. Guo, Simultaneous removal of antibiotic resistant bacteria, antibiotic resistance genes, and micropollutants by a modified photo-Fenton process, Water Res. 197 (2021), 117075, https://doi.org/10.1016/j.watres.2021.117075.

[25] M.A. Prada-Vásquez, S.E. Estrada-Flórez, E.A. Serna-Galvis, R.A. Torres-Palma, Developments in the intensification of photo-Fenton and ozonation-based processes for the removal of contaminants of emerging concern in Ibero-American countries, Sci. Total Environ. 765 (2021), 142699, https://doi.org/10.1016/j.scitotenv.2020.142699.

[26] L. Xu, J. Wang, A heterogeneous Fenton-like system with nanoparticulate zero-valent iron for removal of 4-chloro-3-methyl phenol, J. Hazard. Mater. 186 (2011) 256–264, https://doi.org/10.1016/j.jhazmat.2010.10.116.

[27] Y. Segura, F. Martínez, J.A. Melero, Effective pharmaceutical wastewater degradation by Fenton oxidation with zero-valent iron, Appl. Catal. B Environ. 136–137 (2013) 64–69, https://doi.org/10.1016/j.apcatb.2013.01.036.

[28] H. Hansson, F. Kaczala, M. Marques, W. Hogland, Photo-Fenton and Fenton oxidation of recalcitrant industrial wastewater using nanoscale zero-valent iron, Int. J. Photoenergy. 2012 (2012), https://doi.org/10.1155/2012/531076.

[29] X. Cheng, S. Wang, W. Huang, F. Wang, S. Fang, R. Ge, Q. Zhang, L. Zhang, W. Du, F. Fang, Q. Feng, J. Cao, J. Luo, Current status of hypochlorite technology on the wastewater treatment and sludge disposal: performance, principals and prospects, Sci. Total Environ. 803 (2022), 150085, https://doi.org/10.1016/j.scitotenv.2021.150085.

[30] M. Pirsaheb, S. Moradi, M. Shahlaei, X. Wang, N. Farhadian, A new composite of nano zero-valent iron encapsulated in carbon dots for oxidative removal of bio-refractory antibiotics from water, J. Clean. Prod. 209 (2019) 1523–1532, https://doi.org/10.1016/j.jclepro.2018.11.175.

[31] S. Zha, Y. Cheng, Y. Gao, Z. Chen, M. Megharaj, R. Naidu, Nanoscale zero-valent iron as a catalyst for heterogeneous Fenton oxidation of amoxicillin, Chem. Eng. J. 255 (2014) 141–148, https://doi.org/10.1016/j.cej.2014.06.057.

[32] J. Scaria, A. Gopinath, P.V. Nidheesh, A versatile strategy to eliminate emerging contaminants from the aqueous environment: heterogeneous Fenton process, J. Clean. Prod. 278 (2021), 124014, https://doi.org/10.1016/j.jclepro.2020.124014.

[33] A. Babuponnusami, K. Muthukumar, Treatment of phenol-containing wastewater by photoelectro-Fenton method using supported nanoscale zero-valent iron, Environ. Sci. Pollut. Res. 20 (2013) 1596–1605, https://doi.org/10.1007/s11356-012-0990-1.

[34] M. Alizadeh Fard, A. Torabian, G.R.N. Bidhendi, B. Aminzadeh, Fenton and photo-Fenton oxidation of petroleum aromatic hydrocarbons using nanoscale zero-valent iron, J. Environ. Eng. 139 (2013) 966–974, https://doi.org/10.1061/(ASCE)EE.1943-7870.0000705.

[35] M. Minella, E. Sappa, K. Hanna, F. Barsotti, V. Maurino, C. Minero, D. Vione, Considerable Fenton and photo-Fenton reactivity of passivated zero-valent iron, RSC Adv. 6 (2016) 86752–86761.

[36] M. Kallel, C. Belaid, T. Mechichi, M. Ksibi, B. Elleuch, Removal of organic load and phenolic compounds from olive mill wastewater by Fenton oxidation with zero-valent iron, Chem. Eng. J. 150 (2009) 391–395, https://doi.org/10.1016/j.cej.2009.01.017.

[37] C. Noubactep, Comment on "Oxidative degradation of organic compounds using zero-valent iron in the presence of natural organic matter serving as an electron shuttle", Environ. Sci. Technol. 43 (2009) 3964–3965, https://doi.org/10.1021/es900076m.

[38] H. Barndōk, L. Blanco, D. Hermosilla, Á. Blanco, Heterogeneous photo-Fenton processes using zero valent iron microspheres for the treatment of wastewaters contaminated with 1,4-dioxane, Chem. Eng. J. 284 (2016) 112–121, https://doi.org/10.1016/j.cej.2015.08.097.

[39] G.B. Ortiz De La Plata, O.M. Alfano, A.E. Cassano, 2-chlorophenol degradation via photo Fenton reaction employing zero valent iron nanoparticles, J. Photochem. Photobiol. A Chem. 233 (2012) 53–59, https://doi.org/10.1016/j.jphotochem.2012.02.023.

[40] L. Gomathi Devi, S. Girish Kumar, K. Mohan Reddy, C. Munikrishnappa, Photo degradation of methyl Orange an azo dye by advanced Fenton process using zero valent metallic iron: influence of various reaction parameters and its degradation mechanism, J. Hazard. Mater. 164 (2009) 459–467, https://doi.org/10.1016/j.jhazmat.2008.08.017.

[41] A. Babuponnusami, K. Muthukumar, Removal of phenol by heterogenous photo electro Fenton-like process using nano-zero valent iron, Sep. Purif. Technol. 98 (2012) 130–135, https://doi.org/10.1016/j.seppur.2012.04.034.

[42] Y. Kuang, Q. Wang, Z. Chen, M. Megharaj, R. Naidu, Heterogeneous Fenton-like oxidation of monochlorobenzene using green synthesis of iron nanoparticles, J. Colloid Interface Sci. 410 (2013) 67–73, https://doi.org/10.1016/j.jcis.2013.08.020.

[43] M. Rossier, M. Schreier, U. Krebs, B. Aeschlimann, R. Fuhrer, M. Zeltner, R. N. Grass, D. Günther, W.J. Stark, Scaling up magnetic filtration and extraction to the ton per hour scale using carbon coated metal nanoparticles, Sep. Purif. Technol. 96 (2012) 68–74, https://doi.org/10.1016/j.seppur.2012.05.043.

[44] H. Luo, Y. Zeng, D. He, X. Pan, Application of iron-based materials in heterogeneous advanced oxidation processes for wastewater treatment: a review, Chem. Eng. J. 407 (2021), 127191, https://doi.org/10.1016/j.cej.2020.127191.

[45] J.A. Donadelli, B. Caram, M. Kalaboka, M. Kapsi, V.A. Sakkas, L. Carlos, F.S. García Einschlag, Mechanisms of 4-phenylazophenol elimination in micro- and nano-ZVI assisted-Fenton systems, J. Environ Chem. Eng. 8 (2020), 103624, https://doi.org/10.1016/j.jece.2019.103624.

[46] P. Charalambous, I. Vyrides, In situ biogas upgrading and enhancement of anaerobic digestion of cheese whey by addition of scrap or powder zero-valent iron (ZVI), J. Environ. Manag. 280 (2021), 111651, https://doi.org/10.1016/j.jenvman.2020.111651.

[47] H.S. Son, J.K. Im, K.D. Zoh, A Fenton-like degradation mechanism for 1,4-dioxane using zero-valent iron (Fe0) and UV light, Water Res. 43 (2009) 1457–1463, https://doi.org/10.1016/j.watres.2008.12.029.

[48] E. Khan, W. Wirojanagud, N. Sermsai, Effects of iron type in Fenton reaction on mineralization and biodegradability enhancement of hazardous organic compounds, J. Hazard. Mater. 161 (2009) 1024–1034, https://doi.org/10.1016/j.jhazmat.2008.04.049.

[49] V. Singh, S. Suthar, Occurrence, seasonal variations, and ecological risk of pharmaceuticals and personal care products in river Ganges at two holy cities of India, Chemosphere 268 (2021), 129331, https://doi.org/10.1016/j.chemosphere.2020.129331.

[50] S. Zhu, H. Chen, J. Li, Sources, distribution and potential risks of pharmaceuticals and personal care products in qingshan Lake basin, eastern China, Ecotoxicol. Environ. Saf. 96 (2013) 154–159, https://doi.org/10.1016/j.ecoenv.2013.06.033.

[51] Z. Li, J.K. Kim, V. Chaudhari, S. Mayadevi, L.C. Campos, Degradation of metaldehyde in water by nanoparticle catalysts and powdered activated carbon, Environ. Sci. Pollut. Res. 24 (2017) 17861–17873, https://doi.org/10.1007/s11356-017-9249-1.

[52] L. Wang, J. Yang, Y. Li, J. Lv, J. Zou, Removal of chlorpheniramine in a nanoscale zero-valent iron induced heterogeneous Fenton system: influencing factors and degradation intermediates, Chem. Eng. J. 284 (2016) 1058–1067, https://doi.org/10.1016/j.cej.2015.09.042.

[53] J.K. Yan, Y.Y. Wang, H. Le Ma, Z. Bin Wang, Ultrasonic effects on the degradation kinetics, preliminary characterization and antioxidant activities of polysaccharides from phellinus linteus mycelia, Ultrason. Sonochem. 29 (2016) 251–257, https://doi.org/10.1016/j.ultsonch.2015.10.005.

[54] M.S. Rahman, K.V. Sathasivam, Heavy metal adsorption onto Kappaphycus sp. from aqueous solutions: the use of error functions for validation of isotherm and kinetics models, Biomed. Res. Int. (2015 (2015).), https://doi.org/10.1155/2015/126298.

[55] K. Riahi, S. Chaabane, B. Ben Thayer, A kinetic modeling study of phosphate adsorption onto Phoenix dactylifera L. Date palm fibers in batch mode, J. Saudi Chem. Soc. 21 (2017) S143–S152, https://doi.org/10.1016/j.jscs.2013.11.007.

[56] J. Li, Y. Liu, L.C. Campos, M.-O. Coppens, E. Increased, Coli bio-adsorption resistance of microfiltration membranes, using a bio-inspired approach, Sci. Total Environ. 751 (2021), 141777.

[57] J. Li, Q. Zhou, L.C. Campos, Removal of selected emerging PPCP compounds using greater duckweed (Spirodela polyrhiza) based lab-scale free water constructed wetland, Water Res. 126 (2017) 252–261, https://doi.org/10.1016/j.watres.2017.09.002.

[58] C. Ávila, C. Pelissari, P.H. Sezerino, M. Sgroi, P. Roccaro, J. García, Enhancement of total nitrogen removal through effluent recirculation and fate of PPCPs in a hybrid constructed wetland system treating urban wastewater, Sci. Total Environ. 584–585 (2017) 414–425, https://doi.org/10.1016/j.scitotenv.2017.01.024.

[59] E.S. Elmolla, M. Chaudhuri, Degradation of the antibiotics amoxicillin, ampicillin and cloxacillin in aqueous solution by the photo-Fenton process, J. Hazard. Mater. 172 (2009) 1476–1481, https://doi.org/10.1016/j.jhazmat.2009.08.015.

[60] B.H. Diya'uddeen, S.Rahim Pouran, A.R.Abdul Aziz, S.M. Nashwan, W.M.A. Wan Daud, M.G. Shaaban, Hybrid of Fenton and sequencing batch reactor for petroleum refinery wastewater treatment, J. Ind. Eng. Chem. 25 (2015) 186–191, https://doi.org/10.1016/j.jiec.2014.10.033.

[61] C.H. Liao, S.F. Kang, Y.W. Hsu, Zero-valent iron reduction of nitrate in the presence of ultraviolet light, organic matter and hydrogen peroxide, Water Res. 37 (2003) 4109–4118, https://doi.org/10.1016/S0043-1354(03)00248-3.

[62] M. Ksibi, Chemical oxidation with hydrogen peroxide for domestic wastewater treatment, Chem. Eng. J. 119 (2006) 161–165, https://doi.org/10.1016/j.cej.2006.03.022.

[63] J. He, X. Yang, B. Men, L. Yu, D. Wang, EDTA enhanced heterogeneous Fenton oxidation of dimethyl phthalate catalyzed by Fe3O4: kinetics and interface mechanism, J. Mol. Catal. A Chem. 408 (2015) 179–188.

[64] N. de O. Dos Santos, L. Teixeira, Accelerated reoxygenation of water bodies using hydrogen peroxide, Int. J. Environ. Stud. 76 (2019) 558–570.

[65] A. Babuponnusami, K. Muthukumar, A review on Fenton and improvements to the Fenton process for wastewater treatment, J. Environ. Chem. Eng. 2 (2014) 557–572, https://doi.org/10.1016/j.jece.2013.10.011.

[66] J.J. Pignatello, E. Oliveros, A. MacKay, Advanced oxidation processes for organic contaminant destruction based on the Fenton reaction and related chemistry, Crit. Rev. Environ. Sci. Technol. 36 (2006) 1–84, https://doi.org/10.1080/10643380500326564.

[67] S. Bae, D. Kim, W. Lee, Degradation of diclofenac by pyrite catalyzed Fenton oxidation, Appl. Catal. B Environ. 134–135 (2013) 93–102, https://doi.org/10.1016/j.apcatb.2012.12.031.

[68] F. Velichkova, C. Julcour-Lebigue, B. Koumanova, H. Delmas, Heterogeneous Fenton oxidation of paracetamol using iron oxide (nano)particles, J. Environ. Chem. Eng. 1 (2013) 1214–1222, https://doi.org/10.1016/j.jece.2013.09.011.

[69] R.S. Karale, B. Manu, S. Shrihari, Fenton and photo-fenton oxidation processes for degradation of 3-aminopyridine from water, APCBEE Proc. 9 (2014) 25–29, https://doi.org/10.1016/j.apcbee.2014.01.005.

[70] S. Veloutsou, E. Bizani, K. Fytianos, Photo-Fenton decomposition of β-blockers atenolol and metoprolol; study and optimization of system parameters and identification of intermediates, Chemosphere 107 (2014) 180–186, https://doi.org/10.1016/j.chemosphere.2013.12.031.

[71] M. Anis, S. Haydar, Oxidative degradation of acetaminophen by continuous flow classical fenton process, Desalin. Water Treat. 139 (2019) 166–173, https://doi.org/10.5004/dwt.2019.23278.

[72] N. Klamerth, S. Malato, A. Agüera, A. Fernández-Alba, Photo-Fenton and modified photo-Fenton at neutral pH for the treatment of emerging contaminants in wastewater treatment plant effluents: a comparison, Water Res. 47 (2013) 833–840, https://doi.org/10.1016/j.watres.2012.11.008.

[73] H. Yamamoto, Y. Nakamura, S. Moriguchi, Y. Nakamura, Y. Honda, I. Tamura, Y. Hirata, A. Hayashi, J. Sekizawa, Persistence and partitioning of eight selected pharmaceuticals in the aquatic environment: laboratory photolysis, biodegradation, and sorption experiments, Water Res. 43 (2009) 351–362, https://doi.org/10.1016/j.watres.2008.10.039.

[74] K. Aranami, J.W. Readman, in: Photolytic degradation of triclosan in freshwater and seawater 66, 2007, pp. 1052–1056, https://doi.org/10.1016/j.chemosphere.2006.07.010.

[75] N. Klamerth, L. Rizzo, S. Malato, M.I. Maldonado, A. Agüera, A.R. Fernández-Alba, Degradation of fifteen emerging contaminants at μg L-1 initial concentrations by mild solar photo-Fenton in MWTP effluents, Water Res. 44 (2010) 545–554, https://doi.org/10.1016/j.watres.2009.09.059.

[76] G. Bedoux, B. Roig, O. Thomas, V. Dupont, B. Le Bot, Occurrence and toxicity of antimicrobial triclosan and by-products in the environment, Environ. Sci. Pollut. Res. Int. 19 (2012) 1044–1065, https://doi.org/10.1007/s11356-011-0632-z.

[77] Y. Zhou, B. Xiao, S.Q. Liu, Z. Meng, Z.G. Chen, C.Y. Zou, C.B. Liu, F. Chen, X. Zhou, Photo-Fenton degradation of ammonia via a manganese-iron double-active component catalyst of graphene-manganese ferrite under visible light, Chem. Eng. J. 283 (2016) 266–275, https://doi.org/10.1016/j.cej.2015.07.049.

[78] I. Grčić, S. Papić, K. Žižek, N. Koprivanac, Zero-valent iron (ZVI) Fenton oxidation of reactive dye wastewater under UV-C and solar irradiation, Chem. Eng. J. 195–196 (2012) 77–90, https://doi.org/10.1016/j.cej.2012.04.093.

[79] H. Shemer, Y.K. Kunukcu, K.G. Linden, Degradation of the pharmaceutical metronidazole via UV, Fenton and photo-Fenton processes, Chemosphere 63 (2006) 269–276, https://doi.org/10.1016/j.chemosphere.2005.07.029.

[80] Y. Segura, F. Martínez, J.A. Melero, J.L.G. Fierro, Zero valent iron (ZVI) mediated Fenton degradation of industrial wastewater: treatment performance and characterization of final composites, Chem. Eng. J. 269 (2015) 298–305, https://doi.org/10.1016/j.cej.2015.01.102.

[81] M.R. Taha, A.H. Ibrahim, Characterization of nano zero-valent iron (nZVI) and its application in sono-Fenton process to remove COD in palm oil mill effluent, J. Environ. Chem. Eng. 2 (2014) 1–8, https://doi.org/10.1016/j.jece.2013.11.021.

[82] F. Cattaruzza, D. Fiorani, A. Flamini, P. Imperatori, G. Scavia, L. Suber, A.M. Testa, A. Mezzi, G. Ausanio, W.R. Plunkett, Magnetite nanoparticles anchored to crystalline silicon surfaces, Chem. Mater. 17 (2005) 3311–3316, https://doi.org/10.1021/cm050231a.

[83] K.S. Lin, N. Bin Chang, T.D. Chuang, Fine structure characterization of zero-valent iron nanoparticles for decontamination of nitrites and nitrates in wastewater and groundwater, Sci. Technol. Adv. Mater. 9 (2008) 25015, https://doi.org/10.1088/1468-6996/9/2/025015.

[84] S. Nagoya, S. Nakamichi, Y. Kawase, Mechanisms of phosphate removal from aqueous solution by zero-valent iron: a novel kinetic model for electrostatic adsorption, surface complexation and precipitation of phosphate under oxic conditions, Sep. Purif. Technol. 218 (2019) 120–129, https://doi.org/10.1016/j.seppur.2019.02.042.

[85] J.A. de Lima Perini, R. Fernandes Pupo Nogueira, Zero-valent iron mediated degradation of sertraline - effect of H2O2 addition and application to sewage treatment plant effluent, J. Chem. Technol. Biotechnol. 91 (2016) 276–282, https://doi.org/10.1002/jctb.4705.

[86] N.O. Santos, J.C. Spadotto, I.G. Solórzano, L.C. Campos, L.A. Teixeira, Effective degradation of humic acids in water by zero Fenton process, Microsc. Microanal. 24 (2018) 696–697, https://doi.org/10.1017/s1431927618003975.

[87] N. Santos, J. Spadotto, M. Burke, I. Solórzano, L. Campos, L. Teixeira, Removal of humic acid from natural water by ZVI/H 2 O 2 process, Microsc. Microanal. 25 (2019) 798–799, https://doi.org/10.1017/s1431927619004720.

[88] N.O. Dos Santos, L.A.C. Teixeira, J.C. Spadotto, L.C. Campos, A simple ZVI-Fenton pre-oxidation using steel-nails for NOM degradation in water treatment, J. Water Process Eng. 43 (2021), 102230, https://doi.org/10.1016/j.jwpe.2021.102230.